Bioorganic & Medicinal Chemistry Letters 19 (2009) 803–806

Contents lists available at ScienceDirect

Bioorganic & Medicinal Chemistry Letters

journal homepage: www.elsevier.com/locate/bmcl

Insight into the effects of chiral isomers quinidine and quinine on CYP2D6 inhibition

Chunzhi Ai [a,b], Yan Li [c], Yonghua Wang [d], Yadong Chen [e], Ling Yang [a,b,*]

[a] Lab of Pharmaceutical Resource Discovery, Dalian Institute of Chemical Physics, Chinese Academy of Sciences, 457 Zhongshan Road, Dalian 116023, China
[b] Graduate School of Chinese Academy of Sciences, Beijing 100049, China
[c] School of Chemical Engineering, Dalian University of Technology, Dalian 116012, China
[d] School of Life Science and cBiotechnology, Dalian Fisheries University, Dalian 116023, China
[e] Department of Basic Sciences, China Pharmaceutical University, Nanjing 210009, China

ARTICLE INFO

Article history:
Received 3 June 2008
Revised 20 November 2008
Accepted 4 December 2008
Available online 7 December 2008

Keywords:
Stereoisomer
CYP2D6
Inhibitor
CoMFA
CoMSIA
Docking
Molecular electrostatic potential

ABSTRACT

The distinct inhibitory effects against CYP2D6 enzyme of the stereoisomers quinidine and quinine were investigated in this work by employing various methods, including the comparative molecular field analysis (CoMFA), the comparative molecular similarity indices analysis (CoMSIA), the molecular electrostatic potential (MEP) analysis and the docking method. Several 3D-QSAR models with proper reliability were well established, with a CoMFA model with steric and electrostatic fields exhibiting 0.67, 0.99 and 0.88 of q^2, r^2 and r^2_{pred}, respectively, a CoMSIA model with steric, electrostatic and H-bond acceptor fields displaying 0.72, 0.97 and 0.84 of q^2, r^2 and r^2_{pred}, respectively. These models and related docking results reveal that quinidine binds to CYP2D6 in an inverse orientation as compared with quinine. Moreover, quinidine blocks the entrance of the active pocket of CYP2D6 more closely than quinine does, which explains well why the inhibitory activity of quinidine is of 2 magnitudes larger than quinine. This investigation provides a better understanding of the stereoisomeric effects on the bioactivities of the chiral isomers quinidine and quinine interacting with CYP2D6.

In human cytochrome P450 family, CYP2D6 plays a second major role after CYP3A4 as it mediates the metabolism and clearance of about 30% of the currently marketed drugs.[1,2] The common characteristics of CYP2D6 substrates have been recognized as that they possess at least one basic nitrogen atom with a distance of 5 Å or 7 Å to oxidation site, and a negative molecular electrostatic potential above the planar part of the molecule.[3,4] With some of these basic features quinidine and quinine, two stereoisomeric cinchona alkaloids,[5] are not only CYP2D6 substrates but also found to be CYP2D6 inhibitors with, however, different inhibition effects. As a matter of fact, quinidine shows a potent inhibitory activity of 2-order magnitude larger than quinine does.[6] Therefore, it is possible that the stereoisometric difference of the two molecules influence their bindings to CYP2D6 and, in this way, results in different inhibitory effects.

Once a structure–activity study of quinidine and quinine about their bindings to CYP2D6 was conducted by Hutzler et al.[6] McLaughlin also carried out a research on the critical residues of CYP2D6 interacting with quinidine molecule.[7] However, to our knowledge, there is still no investigation up to now showing the distinguished inhibitory effects of these chiral isomers on CYP2D6 from molecular structure.

In the present work, four computation methods including the Comparative Molecular Field Analysis (CoMFA), Comparative Molecular Similarity Indices Analysis (CoMSIA), Molecular Electrostatic Potential (MEP) surface analysis and Docking approach were applied to investigate the stereoisomeric effects of the two kinds of molecules interacting with CYP2D6. Using SYBYL programs, several CoMFA and CoMSIA models[8–11] of the two series of molecules were generated upon an atom-based alignment corresponding to their inhibitory effects. In order to compare the molecular shapes and the MEPs of the stereoisomers quinidine and quinine, the hybrid functional PBE1PBE[12] method was also employed to optimize their geometries at 6-31G* level, with the CUBEGEN program used to compute their MEP distributions using Gaussian 03 suite.[13] The optimized structures of quinidine and quinine were further docked into the active site of CYP2D6 enzyme (PDB Code: 2F9Q)[14] using Surflex-Dock package.[15,16]

In this work, a whole set of 27 molecules including quinidine, quinine and their analogues binding to P450 2D6 was used for the 3D-QSAR analysis[6] (Fig. 1). The dataset was randomly divided into two sets with a training set of 22 and a test set of 5 molecules. Their pIC_{50} values and molecular structures were shown in the supplemental information.

* Corresponding author. Tel.: +86 0411 84379317; fax: +86 0411 84676961.
E-mail address: yling@dicp.ac.cn (L. Yang).

0960-894X/$ - see front matter © 2008 Elsevier Ltd. All rights reserved.
doi:10.1016/j.bmcl.2008.12.016

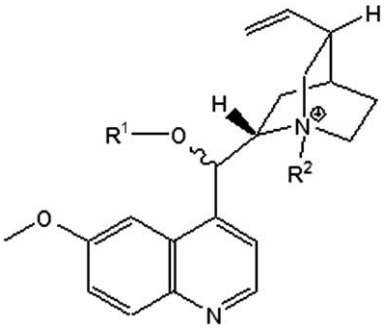

Figure 1. Structure of quinidine/quinine illustrating the substituted sites for analogues. R1 represents the ester/ether formation, and R2 represents the quaternary salt formation.

The CoMFA model was generated from steric and electrostatic fields at the grid lattice of 2 Å. A cross-validated q^2 of 0.67 was yielded based on the leave-one-out partial least squares (PLS) analysis using 6 PLS latent components, with a conventional correlation coefficient r^2 of 0.99. This model was also validated by an independent test set with an excellent r^2_{pred} of 0.88.

Several CoMSIA models were also generated using different descriptors with the optimal models employing the SEA and SEH fields, yet the SEAD model hardly presents any reliability as indicated by the poor predictive performance. The detailed statistic results of the obtained CoMFA and CoMSIA models were shown in the supplemental information.

The predicted and observed pIC_{50} values for the CoMFA (SE) and CoMSIA (SEA, SEH), models are well close to each other within one log unit both in training and test sets as shown in the supplemental information.

Figure 2 shows the generated CoMFA and CoMSIA contour maps. The graphical analysis was made based on the steric (a), electrostatic (b), hydrophobic (c) and hydrogen bond acceptor (d) fields. In Figure 2a, a bulky-disfavored yellow plot is located at the chiral center close to the hydroxyl group of quinidine, indicating that the inhibitory activity of quinidine will be decreased if the hydroxyl was esterified with bulky group. The esters of quinidine (compounds **2**–**8**) all exhibit smaller bioactivities than quinidine does. However, no linear correlation was observed between the size of the bulky substituents and their activities. No contours being observed around the hydroxyl of quinine reveals that the inhibition potency could be hardly influenced by bulky substituents. Accordingly, the esters of quinine (compounds **18**–**22**) all exhibit equivalent bioactivities with quinine except the acetyl ester (compound **17**) that might bind with CYP2D6 in a distinct conformation.

The addition of functional group to nitrogen for quinidine to become the quaternary salt is unfavorable (Fig. 2a), which was conformed by the experimental results that the activities of quaternary salt analogues (compounds **10**–**15**) are in the same magnitude as that of quinidine. A small green plot was found near the basic nitrogen of quinine, indicating that large bulky substitution at this site reduces its inhibitory activity. This explains why the activities of compounds **23**–**27** decreased as the additional bulk increases.

In Figure 2b, a red plot and a blue map were found around the hydroxyl group at the chiral position of quinidine and quinine, respectively. The red region indicates that an ionic interaction or hydrogen-bonding interaction between C(9) hydroxyl region and the amino residue might exists when the molecule binds to CYP2D6. This ionic interaction is usually a strong factor enhancing the molecular interactions, thus, it is reasonable that the activities of compounds **5**–**8**, four quinidine analogues with ester substituents instead of the –OH at C(9) position like quinidine, increase gradually with the richening electron density of these substituents. However, compared with quinidine itself, all ester analogues of quinidine exhibit lower inhibition potencies. All these hint us that when quinidine derivatives bind to CYP2D6, their interaction at

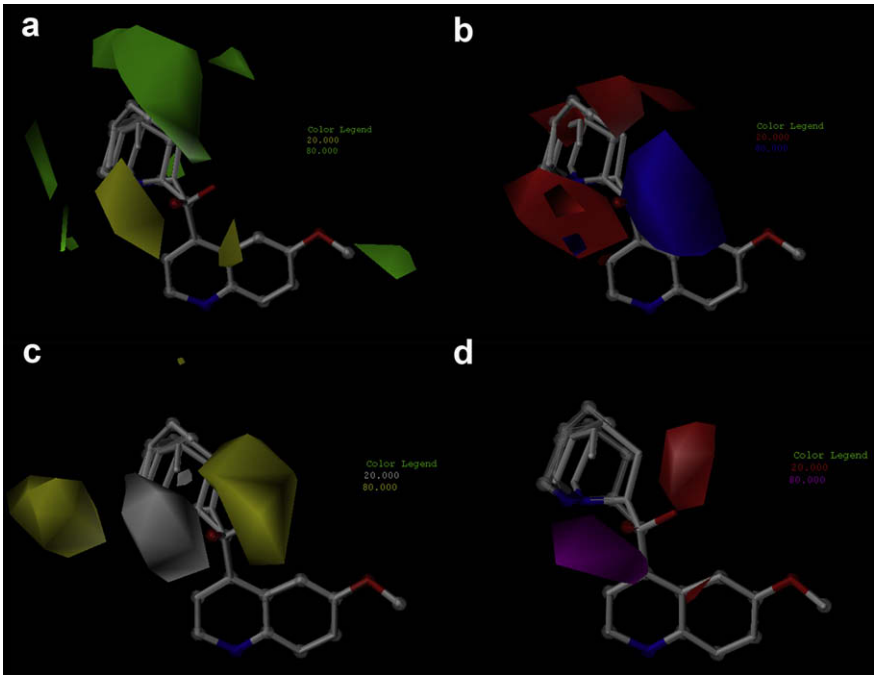

Figure 2. The view of the generated CoMFA and CoMSIA models. Quinidine and quinine were superimposed for visual clarity. Quinidine was shown in stick ball and quinine in capped stick. The color of contours are coded in the following manner: (a) green and yellow represent a region of favorable and unfavorable steric (bulk) interactions, respectively; (b) blue and red indicate electrostatic interactions with a positive charge and a negative charge respectively; (c) yellow and grey represent the hydrophobic and hydrophilic interactions respectively; (d) magenta and red denote the interactions with H-bond acceptor and donor, respectively.

C(9) position with the enzyme depends on the specific substituent at this position. That is, if it is a C(9)–OH group the H-bonding interaction may happens, while if it is a C(9)-ester group the molecule may interact with aminophenol via ion pair. The hydrogen is more electropositive than any acyl group, therefore, the potency of quinine was improved barely when the hydroxyl is esterified.

The electronegative red map is also close to the nitrogen atom of quinidine and quinine, suggesting that the bioactivity would not be increased in case of the basic quinuclidine nitrogen was positively charged. Thereafter, the quaternary salt analogues of quinidine (with positive charge at the nitrogen atom position) did not show any difference in inhibition potency from quinidine. Hutzler et al. assumed that either less inhibition would be observed due to steric interference of the additional N-substituted functional groups in quinidine or perhaps an increase due to the permanent positive charge on the nitrogen, as opposed to a pH-dependent protonation state.[6] We suppose another factor might also be considered—the intramolecular hydrogen bond for the tertiary quinuclidine nitrogen. As for quinine, without the steric interference or the intramolecular hydrogen bond, the inhibitory potency was influenced substantially according to the alkylation of the quinine tertiary quinuclidine nitrogen. The red contour indicates that the substituents with small electronegativity would weaken the inhibitory bioactivity, such as compounds **23**–**25**.

A hydrophilic favored grey area was observed in Figure 2c that located beside the C(9) hydroxyl group of quinidine, suggesting the potency could be improved in the case of hydrophilic substituents. Compared with ester substituents, hydroxyl is a much stronger hydrophilic group which might be a factor that contributes to the higher potency of quinidine than those of its esters. It also interprets the highest IC_{50} values of compounds **3** and **4** which possess the most hydrophobic replacement of C(9) hydroxyl. Contrarily, for quinine a hydrophobic favored yellow polyhedron was situated on the C(9) hydroxyl group, indicating that hydrophobic groups here enhance the inhibitory bioactivity. This could be associated with the stronger potencies for quinine analogues substituted with benzyl-like groups (compounds **18**–**22**) than the compound esterified with acetyl (compounds **17**). The hydrophobic analysis also leads us to conjecture that quinidine binds to the active site of CYP2D6 in a different mode from quinine.

It has been speculated by the electrostatic analysis that H-bond might play a significant role for quinidine to be a potent CYP2D6 inhibitor. The H-bond acceptor contours in Figure 2d confirmed the speculation. The magenta field demonstrates that the C(9) hydroxyl of quinidine forms a hydrogen bond with H-bond acceptor group. Thereafter it is explainable that the inhibitory potency of quinidine was reduced dramatically when the C(9) hydroxyl was esterified with acyls (compounds **2**–**8**) that destroyed the H-bond with residues. Whereas the red plot suggests that the C(9) hydroxyl of quinine does not interact with any H-bond acceptor. That is why the esters of quinine exhibit tiny difference of potency from quinine. So the H-bond formation between C(9) hydroxyl and residue plays as significant role as the electrostatic interactions between the tertiary quinuclidine nitrogen and electronegative groups for the best binding of quinidine with CYP2D6. However, quinine adopts another pose while binding with CYP2D6, as a result, the potency of quinine distinguishes from quinidine in 2 magnitudes.

The optimized geometries of quinidine and quinine were shown in Figure 3, upon which the MEPs were also generated. The MEP maps was interpolated on the electron density surface with values ranging from -30 kcal mol^{-1} (orange) to 30 kcal mol^{-1} (blue), as seen in Figure 4. The chiral differences of quinidine and quinine resulted in their different shape and electrostatic potential maps. In Figure 3, it could be found that the optimized structure of quinidine is stabilized by an intramolecular hydrogen bond between C(15)–H(21) and the tertiary amino N(1), giving a N(1)...H(21) distance of 2.34 Å. Comparably, for quinine this distance turned to be 4.08 Å and no intramolecular hydrogen bond could be formed. Thereafter, the intramolecular hydrogen bond could be used to explain the distinguished correspondence of the isomers in the inhibitory bioactivity to the addition of group to the tertiary amino nitrogen. Quinidine and quinine also share different MEP surface that the MEP of quinidine is flat whereas that of quinine seems bulkily steric. A negative potential band was placed across the aromatic rings of quinidine and quinine. Distinguished from quinidine, quinine shows another negative value of potential at the tertiary quinuclidine nitrogen. The distinct molecular shape and

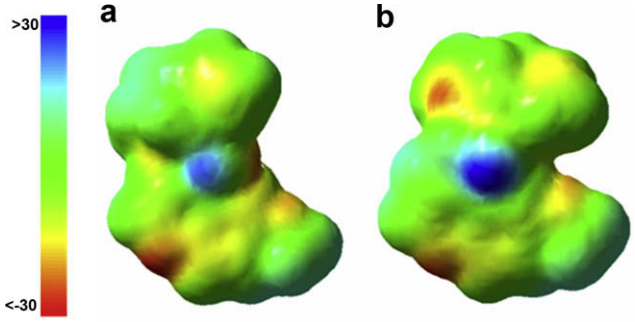

Figure 4. Molecular electrostatic potentials plotted onto the total electron density surface (0.0004e/au^3) for quinidine (a) and quinine (b). The orange color corresponds to a potential of -30 kcal mol^{-1} and the blue color denotes a potential of +30 kcal mol^{-1}.

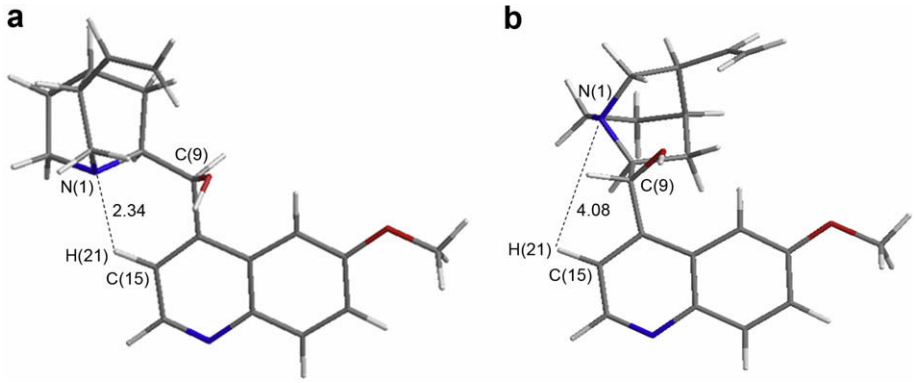

Figure 3. Optimized molecular geometries of quinidine (a) and quinine (b) at PBE1PBE/6-31G* (bond length/Å).

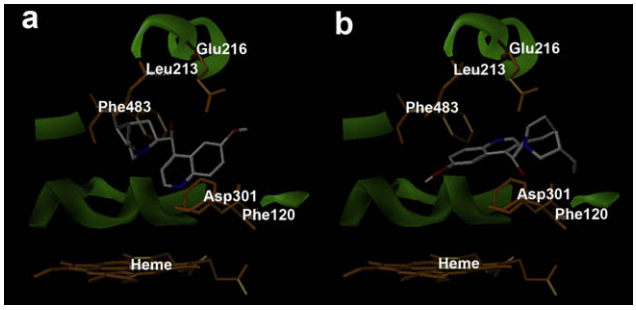

Figure 5. Binding modes of quinidine (a) and quinine (b) with the active site of CYP2D6.

electrostatic potentials of the stereoisomers would contribute greatly to the different binding modes with CYP2D6.

The optimized structures of quinidine and quinine were also docked into the defined protocol of CYP2D6 to explore the possible binding modes, see Figure 5. As a result, the best ranked poses of the isomers were all positioned away from the heme whose smallest distance with heme were 6.5 Å and 5.2 Å and the chemscores were −35.67 and −34.52, respectively. The orientation of quinidine indicates that no site in the molecule could be metabolized by the heme, which is in accordance with the reported experimental results.[7] Phe120 and Phe483 construct a hydrophobic center to interact with the aromatic ring system. Glu216, a carboxylate residue, forms a hydrogen bond with the C(9) hydroxyl, which demonstrates why the bioactivity decreased when the esterification occurred. The geometry of the docked pose varied little from the initial structure of quinidine that was still stabilized with intramolecular H-bond between the tertiary quinuclidine nitrogen (N(1)) and C(1)–H(15). For this reason, the addition of certain substructures to tertiary nitrogen would not affect the inhibitory activity. Quinidine was positioned right above the porphyrin ring, and the entrance of the CYP2D6 active site formed with Leu213 and Phe483 was blocked out with the quinuclidine substructure that other small molecules were prevented from entering the cavity. Distinct from quinidine, quinine placed itself with a reverse pose in the active pocket. Its aromatic ring system still interacts with the hydrophobic residue Phe120 but away from Phe483. No interaction was found between the C(9) hydroxyl of quinine and Glu216. However, the C(9) hydroxyl acts as H-bond accepter to interact with $-NH_2$ of Asp301, suggesting that the esterification of quinine wouldn't destroy the hydrogen bond and accordingly couldn't affect its inhibitory activity. Without the molecular hydrogen bond, the bioactivity would be influenced by the change of electrostatic property due to the alkylation of the tertiary quinuclidine nitrogen. The interspace around the tertiary nitrogen hints us that a bulky addition would be favored to stabilize the binding with CYP2D6. The orientation of quinine only partially blocks the entrance to the active site of CYP2D6, which might be the reason that quinine shows much weaker inhibitory effect than quinidine. The different electrostatic potential surfaces of the stereoisomers determine the distinguished binding tropisms in the active site of CYP2D6.

In this investigation, several established CoMFA and CoMSIA 3D-QSAR models indirectly reflected the information of the active site of CYP2D6 interacting with stereoisomers quinidine and quinine, which was then confirmed by the docking results. The effect of the esterification of C(9) hydroxyl on the inhibitory efficacy mainly depends on the spatial orientation of the stereoisomers in the active site of CYP2D6. Quinidine was disfavored of the bulky esterification of C(9) hydroxyl according to its interaction with the H-bond acceptor residue Glu216, whereas the inhibition of quinine was not influenced by the esterification because its hydroxyl acts as an H-bond acceptor to interact with Asp301. The binding orientation of quinidine generated by docking method is consistent with the docking results reported by McLaughlin et al.[7] The relationship between the bioactivity and the alkylation of tertiary nitrogen relies on whether an intramolecular hydrogen bond was formed or not between N(1) and H(21)–C(15). Quinidine was stabilized by this intramolecular H-bond between N(1) and H(21)–C(15) that drives the quinuclidine charged positively. Comparatively, there is no intramolecular H-bond in quinine, but the alkylation makes quinine charge positively and influences its bioactivity. The positively charged tertiary nitrogen also prefers bulky substitution, thus stabilizing the binding state due to the space effects around the nitrogen. Quinidine blocks the entrance of the active site of CYP2D6 with its quinuclidine substructure, whereas quinine adopts an inverse binding pose which keeps the entrance open. This should be the major factor determining why the quinidine shows a 2-magnitude higher inhibitory effect on CYP2D6 than quinine. These results would provide a better understanding of the stereochemistry's significant roles in the bioactivities of the chiral isomers quinidine and quinine interacting with CYP2D6.

Acknowledgments

This work was supported by the grants from the Key Project of Chinese National Programs for Fundamental Research and Development of 973 Program (No. 2009CB522808) and the Greeting Fund (No. K2006A23) of Dalian Institute of Chemical Physics, Chinese Academy of Sciences.

Supplementary data

Supplementary data associated with this article can be found, in the online version, at doi:10.1016/j.bmcl.2008.12.016.

References and notes

1. Anzenbacher, P.; Anzenbacherová, E. *Cell. Mol. Life Sci.* **2001**, *58*, 737.
2. Ingelman-Sundberg, M. *Trends Pharmacol. Sci.* **2004**, *25*, 193.
3. Koymans, L.; Vermeulen, N. P.; van Acker, S. A.; te Koppele, J. M.; Heykants, J. J.; Lavrijsen, K.; Meuldermans, W.; Donné-Op den Kelder, G. M. *Chem. Res. Toxicol.* **1992**, *5*, 211.
4. Strobl, G. R.; von Kruedener, S.; Stöckigt, J.; Guengerich, F. P.; Wolff, T. *J. Med. Chem.* **1993**, *36*, 1136.
5. Hollman, A. *Br. Heart J.* **1991**, *66*, 301.
6. Hutzler, J. M.; Walker, G. S.; Wienkers, L. C. *Chem. Res. Toxicol.* **2003**, *16*, 450.
7. McLaughlin, L. A.; Paine, M. J.; Kemp, C. A.; Maréchal, J. D.; Flanagan, J. U.; Ward, C. J.; Sutcliffe, M. J.; Roberts, G. C.; Wolf, C. R. *J. Biol. Chem.* **2005**, *280*, 38617.
8. Cramer, R. D.; Patterson, D. E.; Bunce, J. D. *J. Am. Chem. Soc.* **1988**, *110*, 5959.
9. Klebe, G.; Abraham, U.; Mietzner, T. *J. Med. Chem.* **1994**, *37*, 4130.
10. Jozwiak, K.; Khalid, C.; Tanga, M. J.; Berzetei-Gurske, I.; Jimenez, L.; Kozocas, J. A.; Woo, A.; Zhu, W.; Xiao, R. P.; Abernethy, D. R.; Wainer, I. W. *J. Med. Chem.* **2007**, *50*, 2903.
11. Ai, C.; Wang, Y.; Li, Y.; Li, Y.; Yang, L. *QSAR Comb. Sci.* **2008**, *27*, 1183.
12. Perdew, J. P.; Burke, K.; Ernzerhof, M. *Phys. Rev. Lett.* **1997**, *78*, 1396.
13. Frisch, M. J.; Trucks, G. W.; Schlegel, H. B.; Scuseria, G. E.; Robb, M. A.; Cheeseman, J. R.; Zakrzewski, V. G.; Montgomery, J. A. Jr.; Stratmann, R. E.; Burant, J. C.; Dapprich, S.; Millam, J. M.; Daniels, A. D.; Kudin, K. N.; Strain, M. C.; Farkas, O.; Tomasi, J.; Barone, V.; Cossi, M.; Cammi, R.; Mennucci, B.; Pomelli, C.; Adamo, C.; CliÀord, S.; Ochterski, J.; Petersson, G. A.; Ayala, P. Y.; Cui, Q.; Morokuma, K.; Malick, D. K.; Rabuck, A. D.; Raghavachari, K.; Foresman, J. B.; Cioslowski, J.; Ortiz, J. V.; Baboul, A. G.; Stefanov, B. B.; Liu, G.; Liashenko, A.; Piskorz, P.; Komaromi, I.; Gomperts, R.; Martin, R. L.; Fox, D. J.; Keith, T.; Al-Laham, M. A.; Peng, C. Y.; Nanayakkara, A.; Challacombe, M.; Gill, P. M. W.; Johnson, B.; Chen, W.; Wong, M. W.; Andres, J. L.; Gonzalez, C.; Head-Gordon, M.; Replogle, E.S., Pople, J.A. (2003).
14. Rowland, P.; Blaney, F. E.; Smyth, M. G.; Jones, J. J.; Leydon, V. R.; Oxbrow, A. K.; Lewis, C. J.; Tennant, M. G.; Modi, S.; Eggleston, D. S.; Chenery, R. J.; Bridges, A. M. *J. Biol. Chem.* **2006**, *281*, 7614.
15. Jain, A. N. *J. Comput. Aided Mol. Des.* **1996**, *10*, 427.
16. Jain, A. N. *J. Med. Chem.* **2003**, *46*, 499.